CrossMark

ORIGINAL ARTICLE

Diffusion bonding of titanium and AA 7075 aluminum alloy dissimilar joints—process modeling and optimization using desirability approach

S. Rajakumar[1] · V. Balasubramanian[1]

Abstract The major difficulty when joining commercially pure titanium (cp-Ti) and aluminum (Al) lies in the existence of formation of oxide films and brittle intermetallics in the bond region. The diffusion bonding (DB) process parameters such as bonding temperature, bonding pressure, and holding time play a major role to determine the joint strength. In this investigation, an attempt was made to develop an empirical relationship to predict the lap shear strength, interface layer thickness, and weld interface hardness of diffusion-bonded cp-Ti–AA 7075 aerospace aluminum alloy, incorporating above said parameters. Response surface methodology (RSM) was applied to optimize the DB process parameters to attain the maximum shear strength, hardness, and optimum interface layer thickness of the joint. Lap shear tensile test was performed to evaluate shear strength of joints. From this investigation, it is found that the bonds fabricated with the bonding temperature of 510 °C, bonding pressure of 17 MPa, and holding time of 37 min yielded maximum shear strength of 87 MPa, hardness of 163 HV, and interface layer thickness of 7 μm, respectively.

Keywords Diffusion bonding · Mechanical · Microstructure · Shear strength · Hardness · Desirability

✉ S. Rajakumar
  srkcemajor@yahoo.com;
  rajakumar.s.9743@annamalaiuniversity.ac.in

  V. Balasubramanian
  visvabalu@yahoo.com

[1] Department of Manufacturing Engineering, Annamalai University, Annamalai Nagar, Tamil Nadu 608 002, India

1 Introduction

Joining commercially pure titanium (cp-Ti) and AA 7075 aluminum alloy is important in the design and manufacture of many parts. The main reasons for application of titanium and aluminum alloys in aircraft structural parts are due to their properties such as high strength-to-weight ratio and good corrosion resistance [1–3]. Mahendran et al. reported about the principal difficulty when joining dissimilar materials lies in the existence of formation of oxide films and brittle intermetallics in the bond region. However, diffusion bonding can be used to join these alloys without much difficulty [4, 5]. The predominant process parameters in DB process are bonding temperature, bonding pressure, and holding time [6]. As diffusion bonding is formed from atomic migration across an interface, there is no metallurgical continuity at the interface and therefore mechanical properties and microstructure in the bond region are not different from the base metal.

Solid-state DB is a process that joins component parts together without the use of secondary phases, solvent, or liquid. DB can be achieved by applying a static pressure to achieve intimate contact for certain amount of time at high temperature, well below the melting temperature of metals [7]. Since DB is done between 40 and 80 % of the melting point of materials, no phase transformation (similar joints) or micro structural changes can occur during welding [8]. Diffusion is promoted by high temperature, since adhesion is necessary for bonding process [9]. Similar and dissimilar materials can be joined by the DB technique. To produce a metallurgical joint between dissimilar metals, a faster diffusion rate between the materials is necessary, which is accomplished by higher bonding temperatures and longer holding times [10].

Response surface methodology (RSM) consists of a group of mathematical and statistical techniques used in the development of an adequate functional relationship between a

Springer

Table 1 Observation of diffusion-bonded cp-Ti/AA 7075

Input parameters	Parameter range	Photographs of samples	Observation	Probable reason
Bonding temperature	< 425 ºC		No bond	This is mainly due to insufficient temperature to cause diffusion of atom is very less
Bonding temperature	> 525 ºC		Deformed	The use of elevated temperature will aid the inter diffusion of atoms across the interface of the bond and assist surface deformation
Bonding pressure	< 5 MPa		No bond	Due to less no of mating surface between Cp Ti/AA7075. This causes the poor bonding
Bonding pressure	> 20 MPa		Deformed	The bonding pressure should be high enough to ensure a tight contact between the joining surfaces. Moreover, it should be sufficient to aid in the deformation of surface asperities
Holding time	< 5 min		No bond	No bonding at below at 5 min holding time. Due to insufficient time
Holding time	> 45 min		Deformed	Excessive holding time may lead to degradation of physical and chemical properties of the bonds

response of interest. One of the main objectives of RSM is the determination of the optimum settings of the control variables that result in a maximum (or a minimum) response over a certain region of interest, R. This requires having a "good"

Table 2 Important diffusion bonding parameters and their levels for Cp-Ti/AA 7075

S. no.	Parameter	Notation	Unit	Levels				
				(−1.414)	(−1)	(0)	(+1)	(+1.414)
1	Bonding temperature	T	°C	425	439.6	475	510.36	525
2	Bonding pressure	P	MPa	5	7.20	13	17.86	20
3	Holding time	t	Min	5	10.86	25	39.14	45

fitting model that provides an adequate representation of the mean response because such a model is to be utilized to determine the value of the optimum. Optimization techniques used in RSM depend on the nature of the fitted model. For first-degree models, the method of steepest ascent (or descent) is a viable technique for sequentially moving toward the optimum response. This method is explained in detail in [11].

Various methods are there to attain desired output through developing mathematical models to specify the relationships between input and output. The RSM is helpful in developing a suitable approximation for the true functional relationship between independent variables and the response variable that may characterize the nature of the joints. Gunaraj et al. suggested that the submerged arc welding (SAW) is used extensively in industries to join metals for the manufacture of pipes of different diameters and lengths. In this work, RSM technique of design of experiment (DOE) has been applied for the selection of the optimum input variables [12]. Elangovan et al. developed a methodology to

determine the optimum welding conditions that maximize the strength of joints produced by ultrasonic welding using RSM coupled with genetic algorithm (GA). The second-order regression model was developed to predict the weld strength using RSM-central composite design for spot and seam welding of 0.3- and 0.4-mm-thick aluminum specimens [13]. Rajakumar et al. allow fabrication of defect-free welds characterized by good mechanical properties. It is well known that the input welding parameters play a major role in determining the weld quality as the process facts have not been disclosed so far. The selection of input parameters to join aluminum alloy is very difficult. RSM is a collection of mathematical and statistical techniques useful for the modeling and analysis of problems in which a response of one interest is influenced by several variables and the objective is to optimize this response [14].

From the literature review, it is understood that the reported literature [15–20] on DB of cp-Ti–AA 7075 aluminum joints dissimilar materials could be counted

Table 3 Experimental design matrix and responses of Cp-Ti/Al 7075 joints

Joint no.	Coded value			Actual value			SS (MPa)	ILT (μm)	IH (HV)
	T	P	T	T (°C)	P (MPa)	t (min)			
1	+1	+1	−1	510.36	17.80	10.86	80	4.6	140
2	+1	−1	+1	510.36	7.20	39.14	79	5.2	145
3	−1	+1	+1	439.64	17.80	39.14	72	4.5	143
4	−1	−1	−1	439.64	7.20	10.86	70	4.9	147
5	−1.414	0	0	425	12.50	25	70	4.9	145
6	+1.414	0	0	525	12.50	25	81	6	153
7	0	−1.414	0	475	5	25	68	5.1	145
8	0	+1.414	0	475	20	25	77	5.8	152
9	0	0	−1.414	475	12.50	5	73	6.8	149
10	0	0	+1.414	475	12.50	45	79	7.3	155
11	0	0	0	475	12.50	25	74	8.2	162
12	0	0	0	475	12.50	25	75	8	165
13	0	0	0	475	12.50	25	74	8.2	164
14	0	0	0	475	12.50	25	75	8.1	163
15	0	0	0	475	12.50	25	74	8	165

Fig. 1 Flow chart for
optimization steps
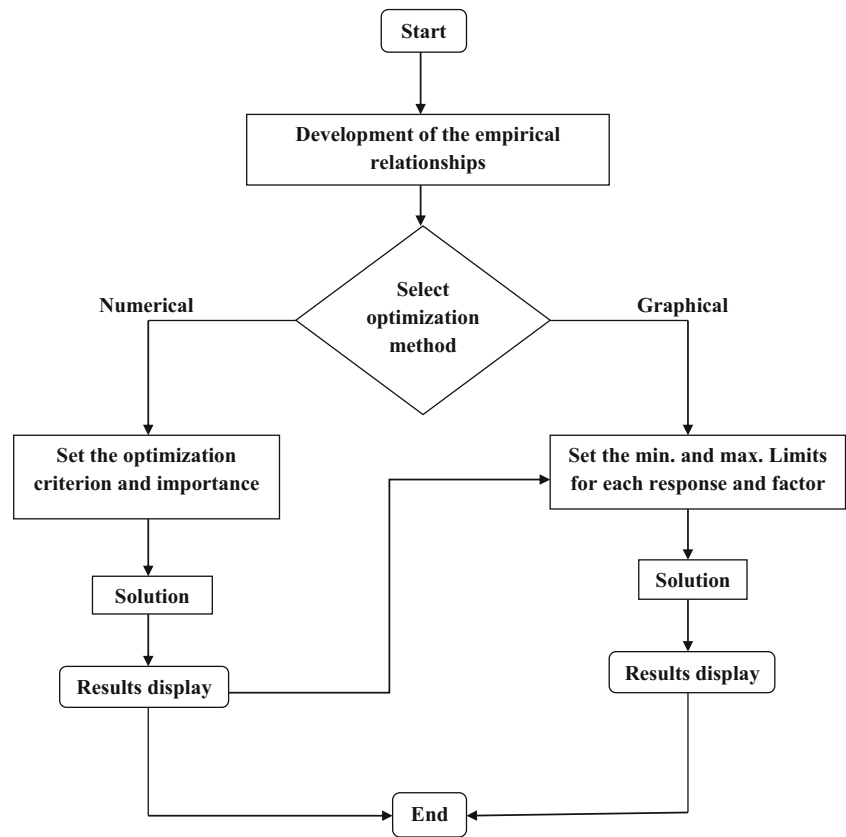
with fingers. Moreover, the available literature is focusing on microstructure analysis, phase formation studies, hardness survey at the interface, and their subsequent influence on bonding strength. No literature was found related to multi-response optimization for DB process parameter of cp-Ti and high strength aerospace aluminum alloy dissimilar joints. The combined effects of process parameters on multi-responses like bonding temperature, bonding pressure, and holding time are hitherto not reported. Hence, in this investigation, an attempt was made to optimize multi-responses of DB process parameters to attain maximum shear strength, interface hardness, and optimum interface layer thickness in cp-

Ti–AA 7075 aluminum alloy dissimilar joints using RSM.

2 Methodology

2.1 Response surface methodology

Engineers often wish to determine the values of the input process parameters at which the responses reach their optimum. The optimum could be either a minimum or a maximum of a particular function in terms of the process input parameters. RSM is a collection of

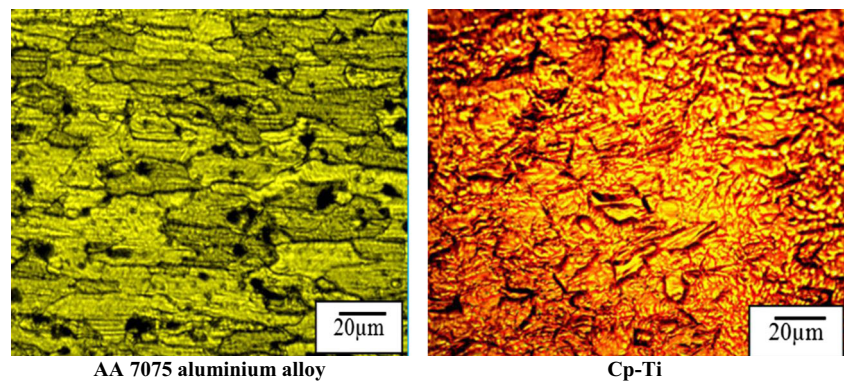**Fig. 2** Base material
microstructures

AA 7075 aluminium alloy   Cp-Ti

Table 4 Chemical composition of the base metals

Base metals	C	Mg	Si	Cr	Mn	Fe	Cu	Zn	O	N	H	Ti	Al
cp-Ti (grade 2)	0.08	–	–	–	–	0.30	–	–	0.25	0.03	0.0015	Bal	–
AA 7075	–	2.1	0.58	0.15	0.12	0.35	1.2	5.1	–	–	–	0.2	Bal.

mathematical and statistical technique useful for analyzing problems in which several independent variables influence a dependent variable or response, and the goal is to optimize the response [21]. In many experimental conditions, it is possible to represent the independent factor in quantitative form as given in Eq. 1. Then, these factors can be thought of having a functional relationship or response as follows:

$$Y = \Phi(x1; x2; \ldots; xk) \pm er \qquad (1)$$

Between the response Y and $x1$, $x2$… xk of k quantitative factors, the function Φ is called response surface or response function. The residual e_r measures the experimental errors. For a given set of independent variables, a characteristic surface is responded. When the mathematical form of Φ is not known, it can be approximated satisfactorily within the experimental region by a polynomial. In the present investigation, RSM was applied for developing the mathematical model in the form of multiple regression equations for the quality characteristic of the DB of cp-Ti–AA 7075. In applying the RSM, the independent variable was viewed as a surface to which a mathematical model is fitted. Representing the lap shear strength of joints by "Y," the response is the function of bonding temperature (T), bonding pressure (P), and holding time (t) and it can be expressed as:

$$Y = f(\text{bonding temperature } (T), \text{ bonding pressure } (P), \text{ and holding time } (t))$$
$$Y = f(T, P, t)$$

The second-order polynomial (regression) equation used to represent the response surface "Y" is given by [22], and the selected polynomial could be expressed as:

$$Y = b_0 + \sum b_i x_i + \sum b_{ii} x_i^2 + \sum b_{ij} x_i x_j + e_r \qquad (2)$$

2.2 Experimental design

The test was designed based on a three-factor, five-level central composite rotatable design with half replication [23]. In order to find the range of each input parameters, trial experiments were performed by changing one of the parameters at a time. Table 1 displays the observation to provide the evidence for fixing the feasible working range of DB parameters. Table 2 shows the process variables, their coded and actual values.

Statistical software Design-Expert V8 was used to code the variables and to establish the design matrix as shown in Table 3. RSM was applied to the experimental data using the same software; polynomial Eq. (2) was fitted to the experimental data to obtain the regression equations for all responses.

2.3 Desirability approach

There are many statistical techniques for solving multiple response problems like overlaying the contour plot for each response, constrained optimization problems, and desirability approach. The desirability method is preferred due to its simplicity and availability in the software and provides flexibility in weighting and giving importance for individual response. Solving such multiple response optimization problems using

Table 5 Physical and mechanical properties of the base metals

Base metals	Crystal structure	Density (g/cc)	Melting point (°C)	Hardness (Hv)	Ultimate tensile strength (MPa)	Yield strength (MPa)	Elongation (%)
cp-Ti (grade 2)	HCP	4.51	1667	142	420	356	20
AA 7075	FCC	2.7	660	160	485	410	12

this technique involves combining multiple responses into a dimensionless measure of performance called the overall desirability function. The desirability approach involves transforming each estimated response, Y_i, into a unit-less utility bounded by $0 < d_i < 1$, where a higher d_i value indicates that response value Y_i is more desirable; if $d_i = 0$, this means a completely undesired response [24]. In the study, the individual desirability of each response, d_i, was calculated using Eqs. 3–6. The shape of the desirability function can be changed for each goal by the weight field "wt_i." Weights are used to give more emphasis to the upper/lower bounds or to emphasize the target value. Weights could be ranged between 0.1 and 10; a weight greater than 1 gives more emphasis to the goal, while weights less than 1 give less emphasis. When the weight value is equal to 1, this will make the d_i vary from 0 to 1 in a linear mode. In the desirability objective function (D), each response can be assigned an importance (r), relative to the other responses. Importance varies from the least important value of 1, indicated by (+), to the most important value of 5, indicated by (+++++). If the varying degrees of importance are assigned to the different responses, the overall objective function is shown in Eq. 7 below, where n is the number of responses in the measure and T_i is the target value of ith response [25].

For the goal of maximum, the desirability will be defined by:

$$d_i = \begin{cases} 0 & Y_i \leq \text{Low}_i \\ \left(\dfrac{y_i - \text{Low}_i}{\text{High}_j - \text{Low}_i}\right)^{wt_i}, & \text{Low}_i < \text{High}_i \\ 1 & Y_i \geq \text{High}_i \end{cases} \quad (3)$$

For the goal of minimum, the desirability will be defined by:

$$d_i = \begin{cases} 1 & Y_i \leq \text{Low}_i \\ \left(\dfrac{\text{High}_i - Y_i}{\text{High}_i - \text{Low}_i}\right)^{wt_i} & \text{Low}_i < Y_i < \text{High}_i \\ 0 & Y_i \geq \text{High}_i \end{cases} \quad (4)$$

For the goal as a target, the desirability will be defined by:

$$d_i = \begin{cases} \left(\dfrac{Y_i - \text{Low}_i}{T_i - \text{Low}_i}\right)^{wt_{1i}} & \text{Low}_i < Y_i < T_i \\ \left(\dfrac{Y_i - \text{High}_i}{T_i - \text{High}_i}\right)^{wt_{2i}} & T_i < Y_i < \text{High}_i \\ 0, & \text{otherwise} \end{cases} \quad (5)$$

For the goal within range, the desirability will be defined by:

$$d_i = \begin{cases} 1, & \text{Low}_i < Y_i < \text{High}_i \\ 0, & \text{otherwise} \end{cases} \quad (6)$$

$$D = \left(\prod_{i=1}^{n} d_i^{r_i}\right)^{1/\sum r_i} \quad (7)$$
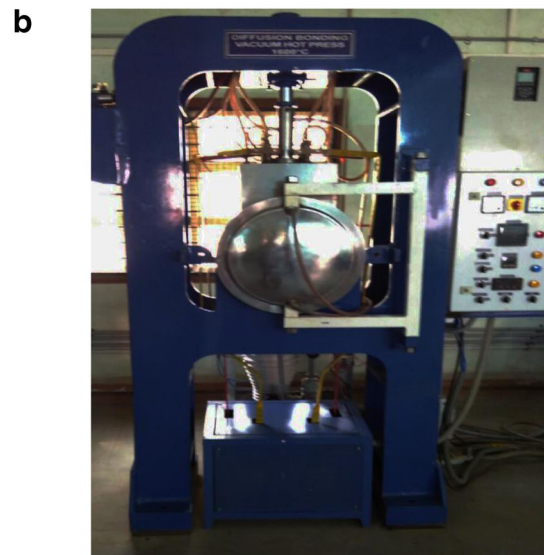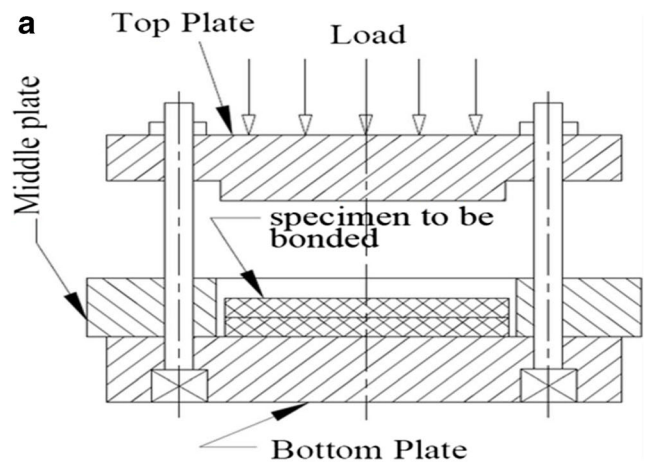
Fig. 3 Experimental details. a Configuration of the diffusion bonding die setup. b Machine setup

2.4 Optimization

The optimization part in Design-Expert software V8 searches for a combination of factor levels that
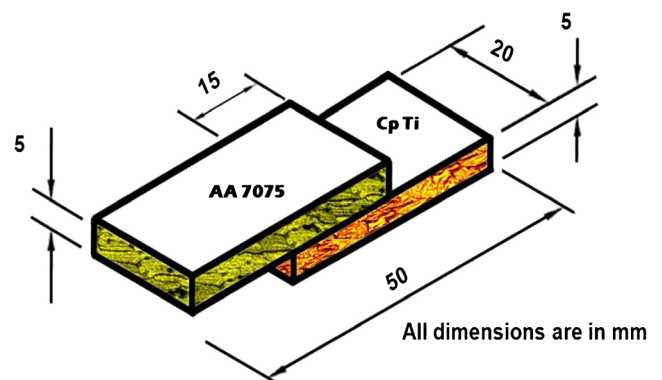

Fig. 4 Dimensions of lap shear tensile test specimens
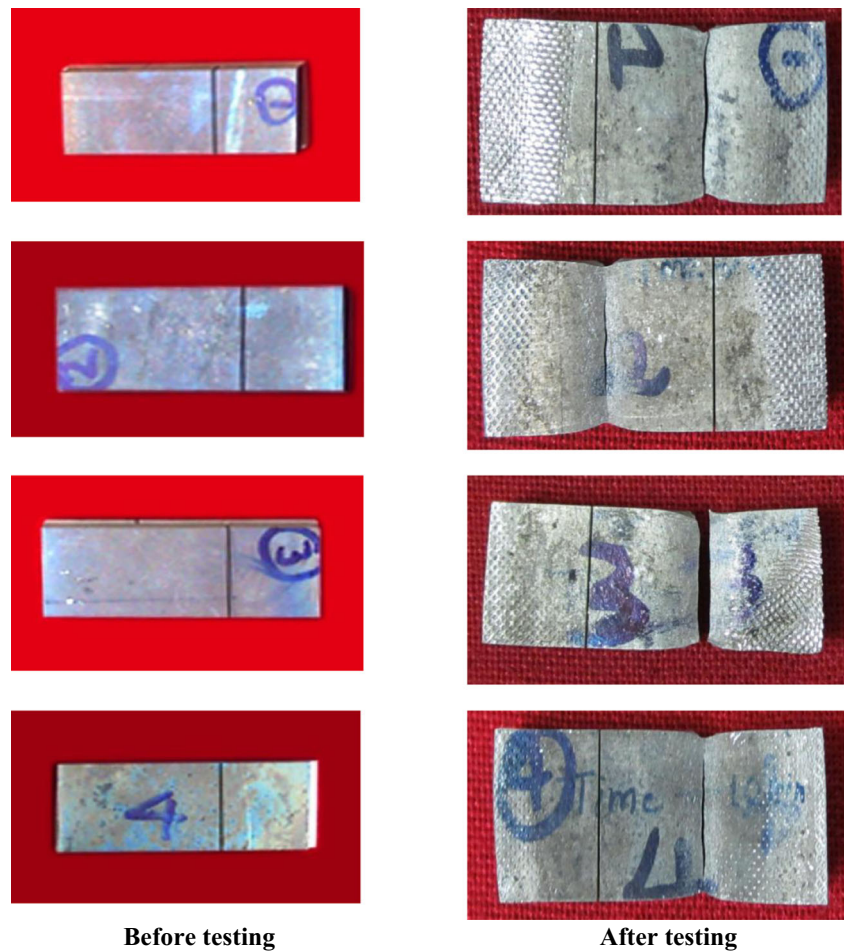
Fig. 5 Lap shear tensile test specimens

| Before testing | After testing |

Table 6 ANOVA test results for cp-Ti/Al 7075 bonds (to identify significant factors)

	Shear strength (SS)		Interface layer thickness (ILT)		Interface hardness (IH)	
	F value	P value Prob > F	F value	P value Prob > F	F value	P value Prob > F
Model	77.5679	<0.0001	267.3271	<0.0001	76.37037	<0.0001
T	201.6667	<0.0001	47.90323	0.0010	20	0.0066
P	135	<0.0001	19.39883	0.0070	15.3125	0.0113
T	60	0.0006	9.897361	0.0255	11.25	0.0202
TP	23.3456	0.0047	2.545178	0.1715	4.3773	0.0906
Tt	39.43019	0.0015	39.19255	0.0015	27.90554	0.0032
Pt	0.868387	0.3942	13.21785	0.0150	20.79196	0.0061
T^2	11.42857	0.0197	1125.448	<0.0001	247.6339	<0.0001
P^2	17.85714	0.0083	1125.448	<0.0001	265.2121	<0.0001
t^2	21.60714	0.0056	189.7801	<0.0001	154.8214	<0.0001
R^2	92 %		95 %		90 %	
Adj. R^2	98.00 %		99.41 %		97.97 %	
Pred. R^2	83.76 %		91.58 %		87.36 %	
Model	Significant		Significant		Significant	

Fig. 6 Normal probability plot of experimental versus predicted. **a** Shear strength. **b** Interface layer thickness. **c** Interface hardness
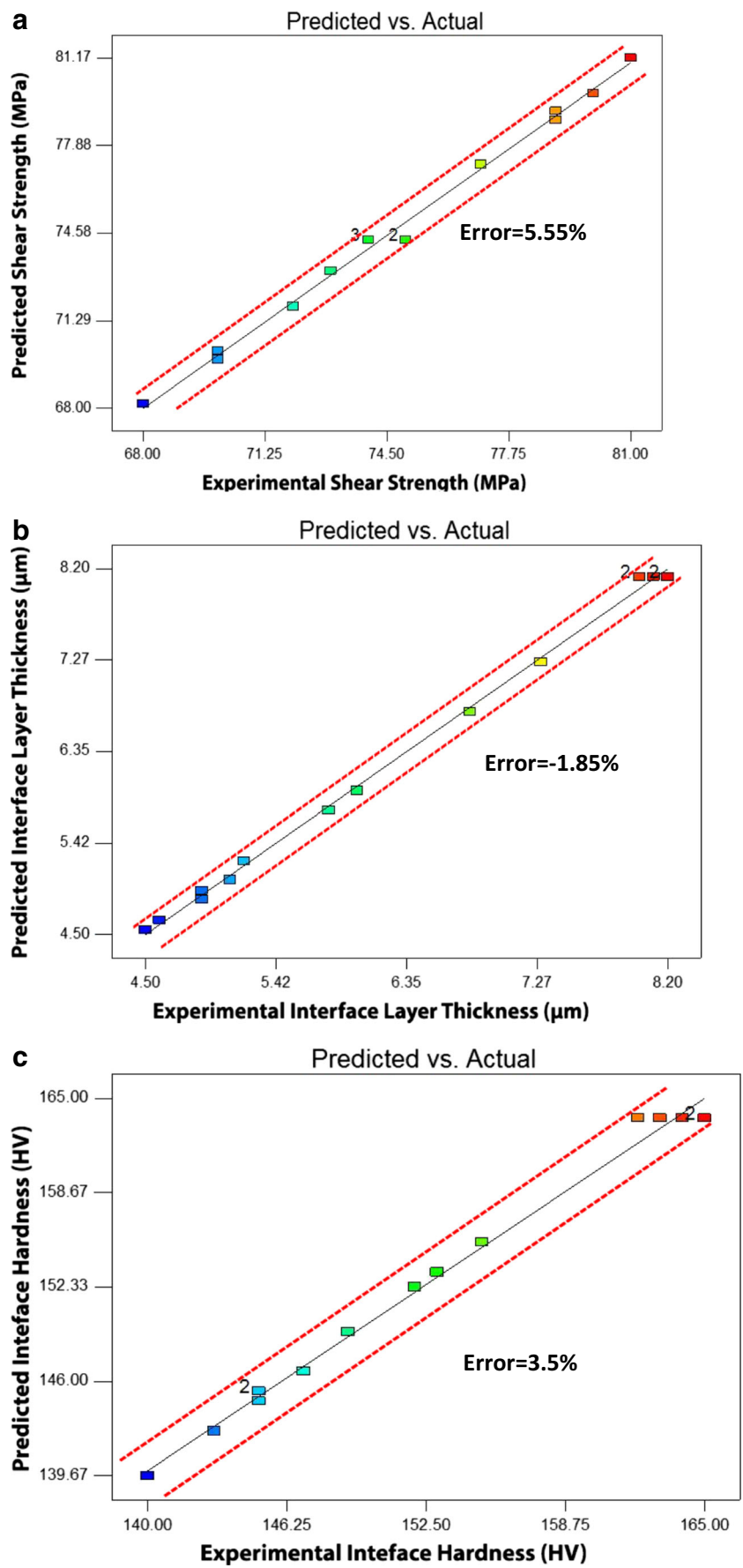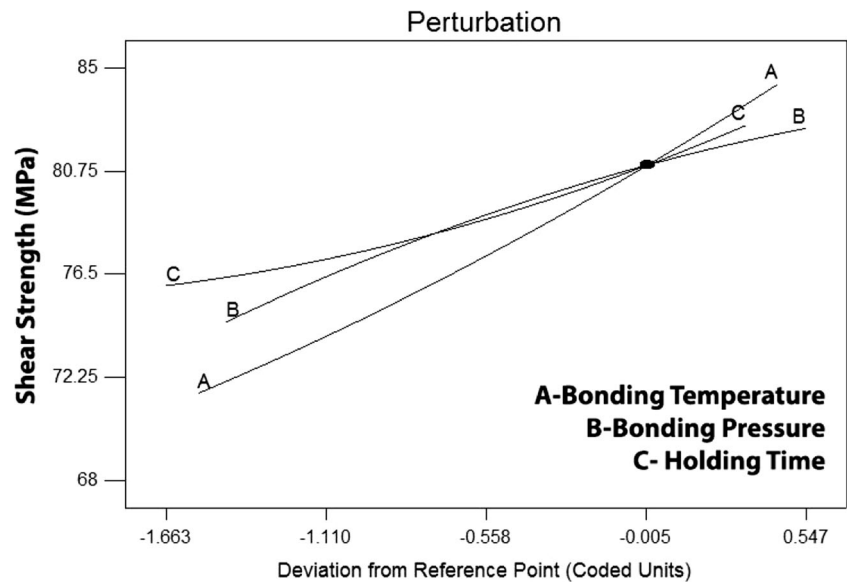
Fig. 7 Perturbation plot sowing the effect of shear strength

simultaneously satisfy the requirements placed (i.e., optimization criteria) on each one of the responses and process factors (i.e., multiple response optimization). Numerical and graphical optimization methods were used in this work by selecting the desired goals for each factor and response. As mentioned before, the numerical optimization process involves combining the goals into an overall desirability function (*D*). The numerical optimization feature in the Design-Expert package finds one point or more in the factor domain that would maximize this objective function. In a graphical optimization with multiple responses, the software defines regions where requirements simultaneously meet the proposed criteria. Also, superimposing or overlaying critical response contours can be defined on a contour plot. Then, a visual search for the best compromise becomes possible. In case of dealing with many responses, it is recommended to run numerical optimization first; otherwise, it could be impossible to find out a feasible region. The graphical optimization displays the area of feasible response values in the factor space, regions that do not fit the optimization criteria are shaded [25]. Figure 1 shows a flow chart of the optimization steps in the Design-Expert software.

3 Experimental work

Square-shaped specimens (50 mm × 50 mm) were machined from rolled plates of 5-mm-thick cp-Ti and AA 7075 materials. Figure 2 reveals the base metal microstructure of cp-Ti and AA 7075 alloys. Kroll's reagent (6 ml HCl, 2 ml HF, and 92 ml water) was used for Ti

alloy, and Keller's reagent made of 5 ml HNO_3 (95 % concentration), 2 ml HF, 3 ml HCl, and 190 ml H_2O was used for Al alloy to reveal the microstructure. The chemical composition and mechanical properties of base metals are presented in Tables 4 and 5, respectively. The polished and chemically treated specimens were stacked in a die. Figure 3a, b shows the configuration of the diffusion bonding die setup inserted into a vacuum chamber (vacuum pressure of −29 mmHg was maintained) and close up view of DB machine setup supplied by VB Ceramics, Chennai Model No. VBCC/DBE/1600° C-01. The specimen was heated up to the bonding temperature using heating furnace with a temperature capacity of 1600 °C; simultaneously, the required pressure was
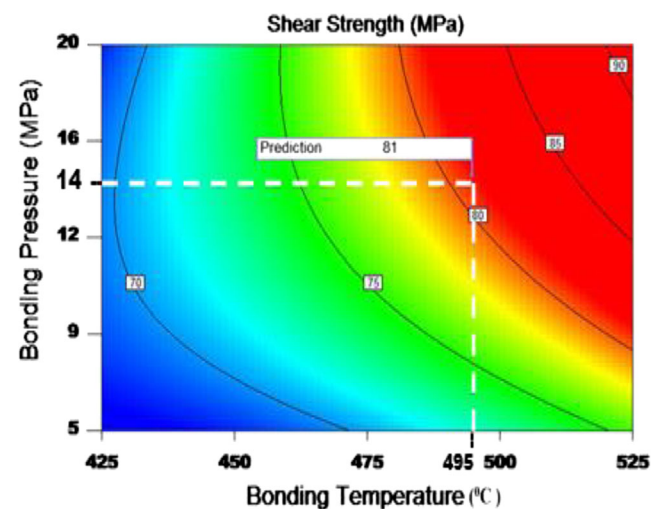

Fig. 8 Contour plot showing the effect of bonding temperature on shear strength

applied. After the completion of bonding, the samples were cooled to room temperature before removing from the chamber. As prescribed by design matrix, 15 joints were fabricated. The lap shear tensile test was performed to evaluate the shear strength of the joints. As the joints were not large enough for normal lap shear strength and bond strength testing, a non-standard test was devised to measure the shear strength of the bonds. The dimensions of lap shear tensile specimens are shown in Fig. 4. The bonded specimens were prepared from the Al/Ti diffusion-bonded joints by a wire cut electric discharge machine (WEDM). The lap shear tensile test and bond strength test were carried out in 100 kN capacity servo-controlled Universal Testing Machine. The images of the specimens before and after the tensile test are shown in Fig. 5. At each experimental condition, three specimens were tested and average of three results is presented in Table 3. Vickers microhardness testing machine (Make: Shimadzu and Model HMV-2T) were employed for measuring the hardness of the bonded region.
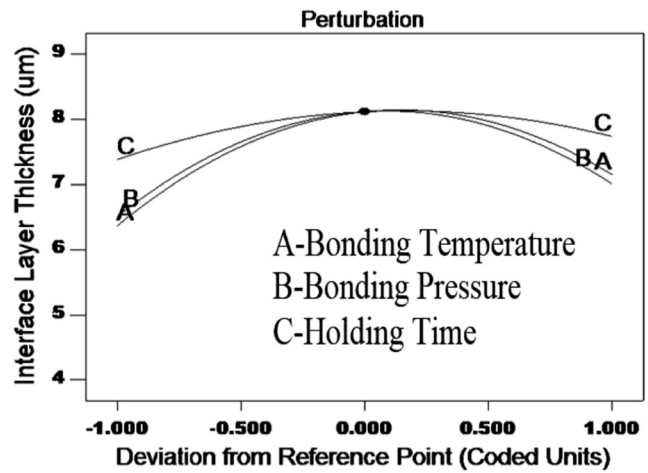

Fig. 10 Perturbation plot sowing the effect of interface layer thickness

3.1 Developing empirical relationships

The response (Y) shear strength (SS) is a function of bonding temperature (T), bonding pressure (P), and holding time (t) and it can be expressed as:

$$SS = f(\text{bonding temperature}(T), \text{ bonding pressure}(P), \text{ and holding time}(t))$$

The second-order polynomial (regression) equation used to represent the response surface "Y," and the selected polynomial could be expressed as

$$\begin{aligned} \text{Shear strength } (SS) = {} & b_0 + b_1(T) + b_2(P) + b_3(t) - b_{11}(T^2) \\ & - b_{22}(P^2) - b_{33}(t^2) + b_{12}(TP) + b_{13}(Tt) \\ & + b_{23}(Pt) \end{aligned} \tag{8}$$

Fig. 9 The XRD result of transition zone on of Ti/Al diffusion bonding
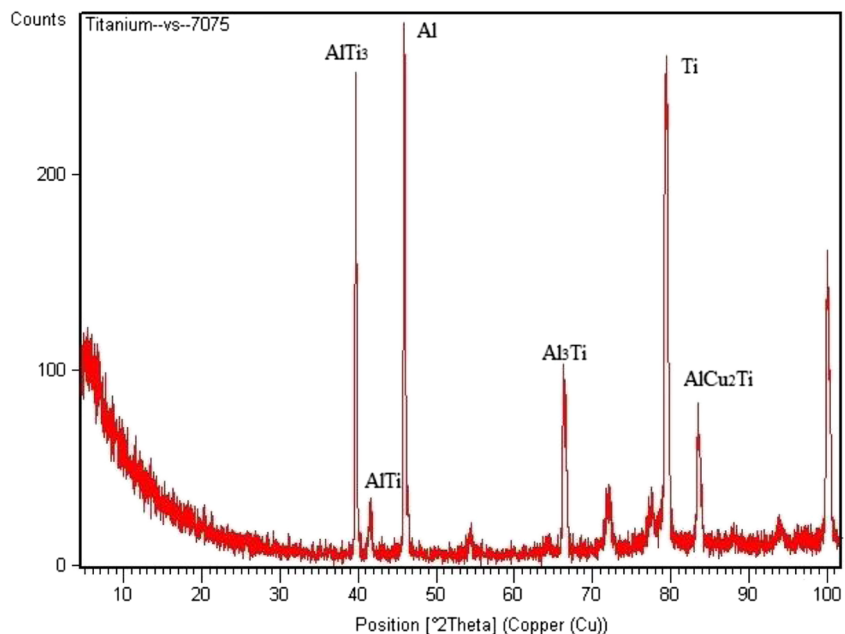
where b_0 is the average of responses b_1, b_2, $b_3 \ldots b_{34}$ which are the coefficients that depend on respective main and interaction factors [21, 22]. In the above expression, all the factors (main and interaction factors) may not have a significant effect on the responses. To identify the significant factors, analysis of variance (ANOVA) test was carried out and the results are presented in Table 6.

Final equations in terms of coded factors are as follows:

$$SS = \{74.33 + 3.89(T) + 3.18(P) + 2.12(t) + 1.87(TP) + 2.43(TH) - 0.36(Pt) + 0.67(T^2) - 0.83(P^2) + 0.92(t^2)\} \text{MPa} \qquad (9)$$

$$\text{Interface layer thickness}(ILT) = \{8.12 + 0.39(T) + 0.254(P) + 0.18(t) + 0.13(TP) + 0.5(TH) + 0.29(Pt) - 1.36(T^2) - 1.36(P^2) - 0.56(t^2)\} \mu\text{m} \qquad (10)$$

$$\text{Interface hardness}(IH) = \{163.67 + 2.83(T) + 2.47(P) + 2.12(t) + 1.87(TP) + 4.72(TH) + 4.08(Pt) - 7.17(T^2) - 7.42(P^2) - 5.67(t^2)\} \text{HV} \qquad (11)$$

The adequacy of the developed empirical relationships was tested using the ANOVA technique [21].

The adequacies of the models so developed were then tested by using the ANOVA, and the results are presented in Table 6. The determination coefficient (R^2) indicates the goodness of fit for the model. In this case, the values of the determination coefficient (R^2) indicate that the model does not explain only less than 5 % of the total variance. The values of the adjusted determination coefficient (adjusted R^2) are also high, which indicates a high significance of the model. From the analysis, it was found that calculated F ratios were larger than the tabulated values at 95 % confidence level; hence, the model is considered to be adequate. Predicted R^2 has also made a good agreement with the adjusted R^2. Adequate precision compares the range of predicted values at the design points to the average prediction error [26]. Each observed response (shear strength, interlayer thickness, and interface hardness) of cp-Ti/Al AA 7075 bonds is compared with the predicted responses calculated from the model, and their respective correlation graphs are presented in Fig. 6a–c. The value of "R^2" for the above-developed relationships are found to be in the range of 90–97 %, which indicates high correlation exists between experimental values and predicted values.

4 Results and discussion

4.1 Shear strength

Perturbation plot shown in Fig. 7 illustrates the effect of DB parameters on the shear strength of an optimized design. This graph shows how the response changes as each factor moves from choosing reference point with all factors held constant as the reference value. Figure 8 contour plot shows that shear strength increases with increasing bonding temperature. It is also evident that the shear strength of the joints closely depends on bonding temperature [27, 28]. At a low temperature of 425 °C, the shear strength of the joints is low. Generally, atoms on either side of the interface can diffuse into the opposite side during the diffusion process only if the temperature is

a Narrow diffusion layer

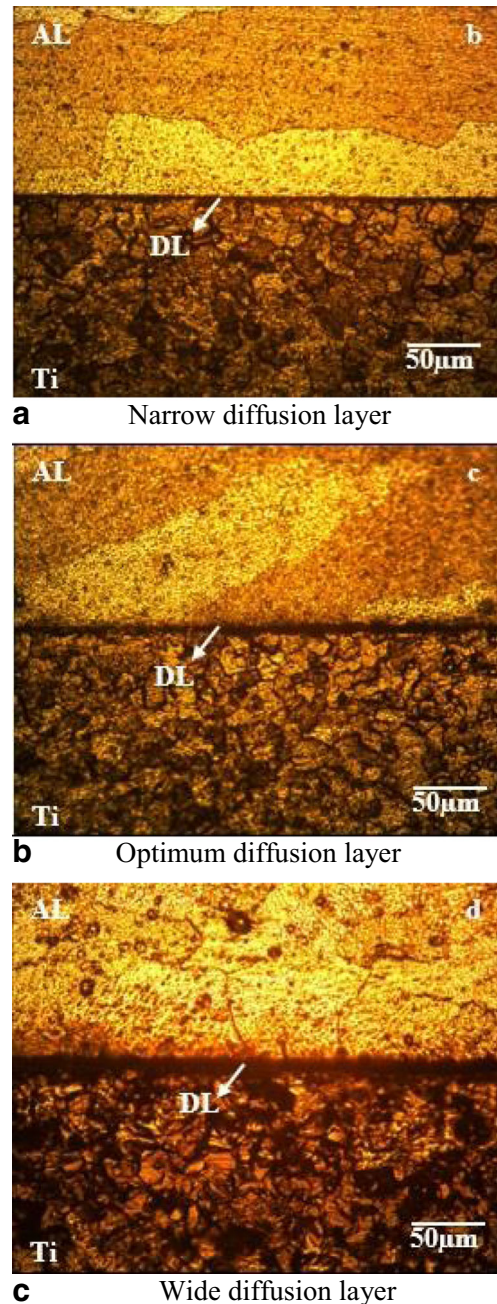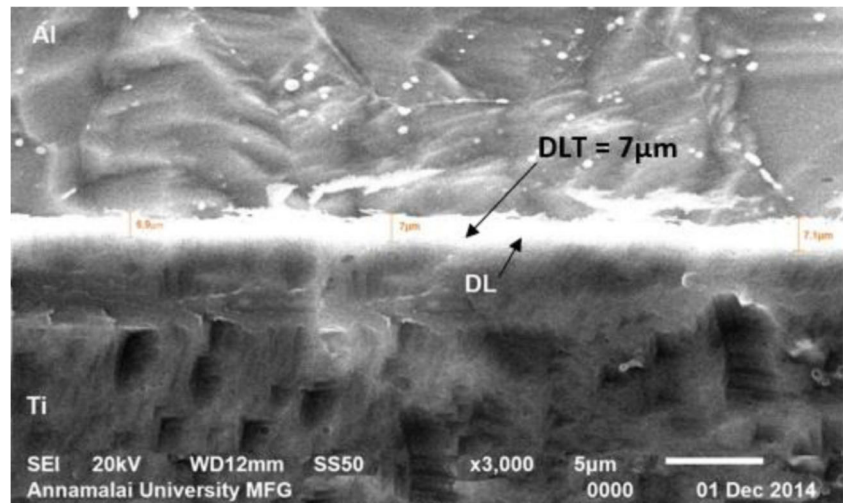**b** Optimum diffusion layer

c Wide diffusion layer

Fig. 11 Optical micrographs of interface region of cp-Ti AA 7075 bonds. **a** Narrow diffusion layer. **b** Optimum diffusion layer. **c** Wide diffusion layer

Fig. 12 SEM measurement of optimum diffusion layer of the interface thickness of cp-Ti/AA 7075 bonds

sufficiently high. So, necessary levels of temperatures are usually in the range of 0.5–0.7 T_m (where T_m represents the melting point of the materials involved). At 400 °C, only a small number of Al atoms might diffuse into the Ti side. This may be the reason for low shear strength. Also, at low temperature, the flowability of metal is substantial yet the yield strength of the base materials remains high, which leads to an incomplete coalescence of the bonding surfaces [29], while increasing in DB temperature 475 °C results in a considerable improvement in shear strength. An increase in DB temperature promotes mass transfer of alloying elements across the interface, which is responsible for the increase in volume fraction of the reaction products and leads to more brittle joints. However, plastic collapse of the bonding surface asperities leads to intimate

contact, which counterbalances the embrittlement due to the intermetallic phases. So, shear strength naturally improves and attains their maximum values. In contrast, at high temperature, the initial stages of bonding could involve migration of interface grain boundaries, and the higher rate of grain growth leads to rapid removal of the bond line and increases the strength near the parent metal [30]. When the bonding temperature reaches 525 °C, the eutectic liquid appears in the interface, and a great quantity of Al elements diffuses into base Ti and forms the intermetallic compounds, which leads the thickness of the intermetallic compound to increase quickly. A quick increase in thickness of intermetallic compound leads to a decrease in the strength and an increase in the brittleness of the joint. With temperatures increasing, the width of

Fig. 13 Contour plot showing the effect of bonding temperature on interface layer thickness
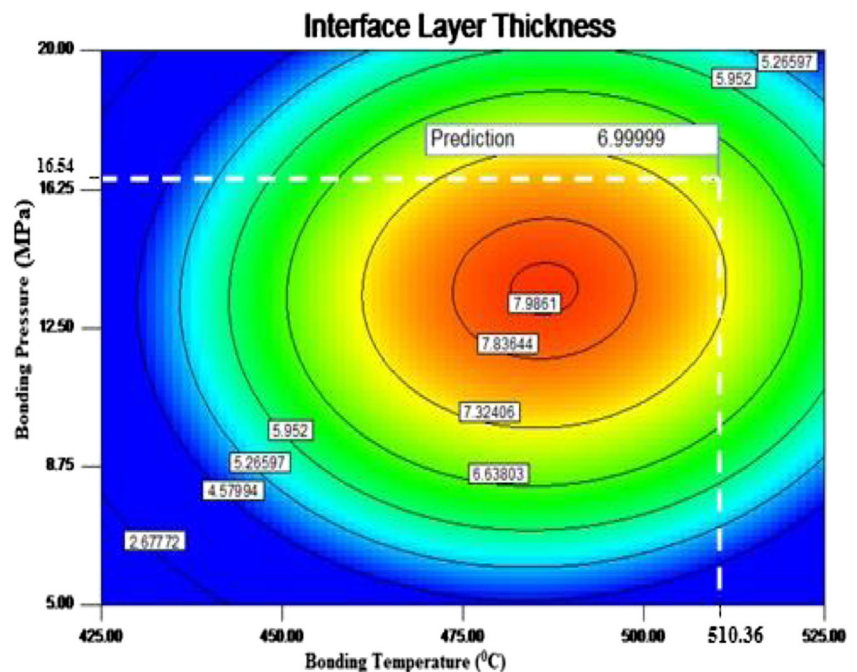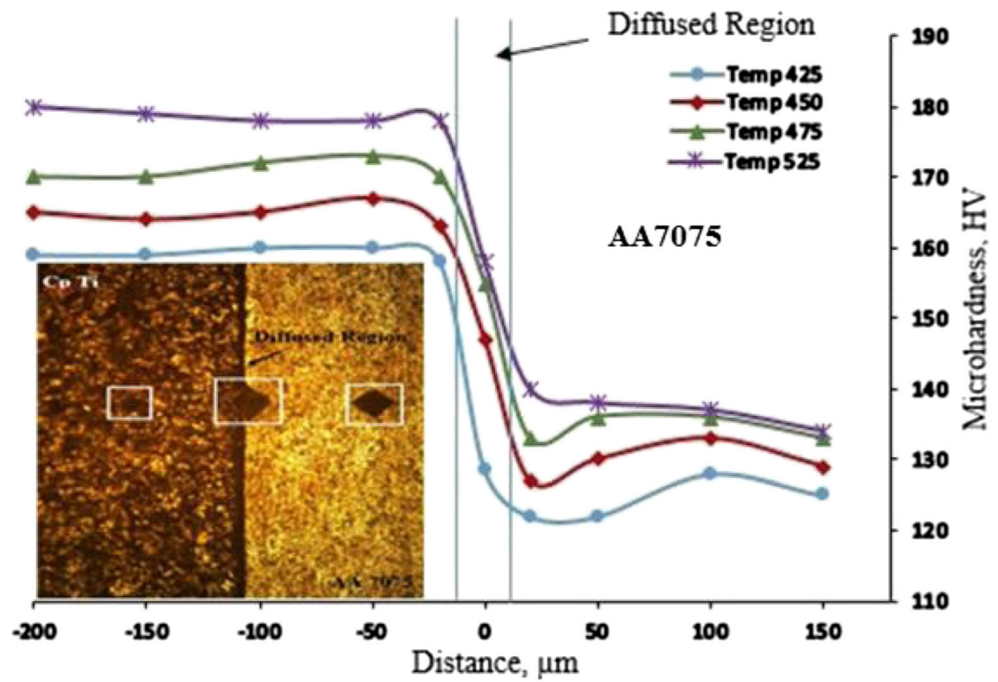
Fig. 14 Microhardness survey across the interface region and indentation mark for optical microstructure

brittle intermetallics considerably increases and the embrittlement effect over-balances the positive effect obtained due to the improvement in coalescence of faying surfaces. As Al-Ti diffusion-bonded joint is a dissimilar joint, the reaction products with new phases are found in the diffusion layer. It is understood that the presence of intermetallics is responsible for low strength. In diffusion bonding between cp-Ti and Al 7075, the highest shear strength value was produced (87 MPa) at the test temperature of 510 °C. From the interface micrographs, the thickness of the intermetallic phase layer was increased by increasing the process parameters. From the predicted model, iterations were carried out to find the optimum intermetallic layer thickness, to achieve maximum lap shear strength. From the results of iterations and experimental results, it is found that intermetallic layer with thickness of 7 μm resulted in higher lap shear strength (87 MPa) irrespective of hardness value. The intermetallic compound grows steadily and gradually at the bond region of dissimilar metal joints with increasing the temperature. The particle distribution of

intermetallic compounds has no harmful effects on the joint performances; moreover, it strengthens the joints. To determine the newly formed phase observed in microstructure, X-ray diffractometry (XRD) was conducted on two sides of the interface. Before the test, the sample was cut off along joining interface surface. The XRD analysis used copper target with 40 kV voltage and 150 mA current. The XRD result of the transition zone on Ti substrate was shown in Fig. 9. Then, diffraction results were compared to JCPDS power diffraction file. The results showed that intermetallics Al_3Ti, $TiAl$, $AlTi_3$, and $AlCu_2Ti$ were formed in the transition zone on Ti substrate and aluminum substrate.

4.2 Interface layer thickness

Perturbation plot shown in Fig. 10 illustrates the effect of DB parameters on the interface layer thickness for an optimized design. This graph shows how the response changes as each factor moves from choosing reference point with all factors

Table 7 Optimization criteria used in this study

Parameter or responses	Limits		Importance	First criterion	Second criterion
	Lower	Upper			
Bonding temperature	425	525	3	Is in range	Maximize
Bonding pressure	5	20	3	Is in range	Is in range
Holding time	5	45	3	Is in range	Is in range
Lap shear strength	68	81	3	Maximize	Maximize
Interface layer thickness	4.5	8.2	3	Is in range	Is target = 7
Interface hardness	140	165	3	Maximize	Maximize

Table 8 Optimal solution as obtained by Design-Expert based on the first criterion (cp-Ti/Al 7075)

|	Experimental details			Response details			
	Input parameters			Response			
Run	Bonding temp (°C)	Bonding pressure (MPa)	Holding time (min)	Lap shear strength (MPa)	Interface layer thickness (μm)	Hardness (HV)	Desirability
1	495	15	34	81	7.923	164.984	1
2	495	15	34	81.001	7.92	164.984	1
3	494	14	34	81	7.926	164.984	1
4	494	14	34	81.003	7.928	164.983	1
5	494	14	34	81.001	7.93	164.982	1
6	495	14	34	81	7.933	164.97	0.999
7	495	14	32	78.23	7.86	160.56	0.99
8	489	13	33	69.56	7.75	159.25	0.99
9	492	15	34	80.2	7.69	159.02	0.99
10	493	13	35	79.58	7.91	155.98	0.99

held constant as the reference value. The interface layer thickness value increases with increasing bonding temperature since the formation of an interface layer at the interface influences the strength of the bond, and it is necessary to analyze the role of interface layer on bonding characteristics. Optical micrographs were taken in the interface region of all the bonds to understand the effect of DB process parameters on the formation of interface layer, and they are presented in Fig. 11a–c. While correlating shear strength results and interface layer thickness, it is concluded that a narrow diffusion layer thickness (Fig. 11a) and relatively wide diffusion layer thickness (Fig. 11c) both lead to minimum shear strength. An optimum interface layer thickness is obtained in Fig. 11b. Figure 12

shows the measured interface layer thickness at middle portion of cp-Ti and AA 7075 dissimilar joints using SEM image. From the SEM image, the average diffusion layer thickness of 7 μm was found to be optimum to obtain higher shear strength. Figure 13 reveals the effect of process parameters on diffusion layer thickness of diffusion-bonded joints. From the contour graphs, the following inferences can be obtained: (1) interface layer thickness increases with increasing the bonding temperature and holding time, and (2) bonding pressure has the least effect when being compared with bonding temperature and holding time. When bonding temperature is taken into consideration, it is seen that interface layer thickness depends mainly on bonding temperature. At 425 °C, the

Table 9 Optimal solution as obtained by Design-Expert based on the second criterion (cp-Ti/Al 7075)

	Experimental details			Response details			
	Input parameters			Response			
Run	Bonding temp (°C)	Bonding pressure (MPa)	Holding time (min)	Lap shear strength (MPa)	Interface layer thickness (μm)	Hardness (HV)	Desirability
1	510	15	37	86.85	6.99	162.7	0.976
2	512	15	37	86.75	7	162.7	0.976
3	512	15	36	86.99	7	162.69	0.976
4	510	15	37	86.66	7.00	162.69	0.976
5	510	15	37	86.53	7.00	162.68	0.976
6	510	15	36	87.21	6.99	162.68	0.976
7	512	15	36	86.39	7.00	162.67	0.976
8	512	15	37	86.62	6.99	162.71	0.975
9	512	15	37	86.04	7.00	162.61	0.975
10	510	15	37	87.25	6.99	162.70	0.972

Fig. 15 Processing maps (overlay) shows the region of optimal bonding condition of cp-Ti/Al7075 (first criterion)
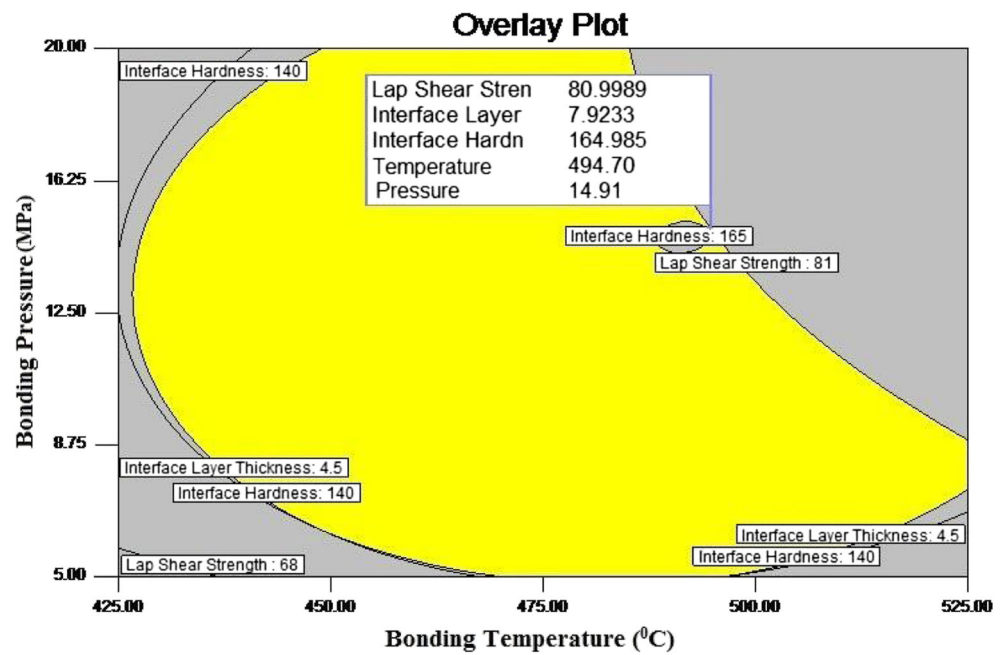
interface layer thickness increases gradually with increasing the bonding temperature. When the bonding temperature reaches to 525 °C, interface layer thickness reaches the maximum. The thickness of diffusion layer depends on atom diffusion [31]. When the bonding temperature increases to over 525 °C, the joining process allows the diffusion of all elements from both metals, which promotes the chemical joint (in all welding condition) between materials when inter-diffusion

between the materials is provided without the formation of voids and brittle phases such as intermetallic compounds. These findings are in agreement with Fick's second law, a partial differential equation describing the rates at which atoms are redistributed in a material by diffusion [32]. The composition, extent, nature, and properties of the phases originated during the welds control the resulting mechanical properties. The intermetallic compound grows steadily and

Fig. 16 Processing maps (overlay) shows the region of optimal bonding condition of cp-Ti/Al7075 (second criterion)
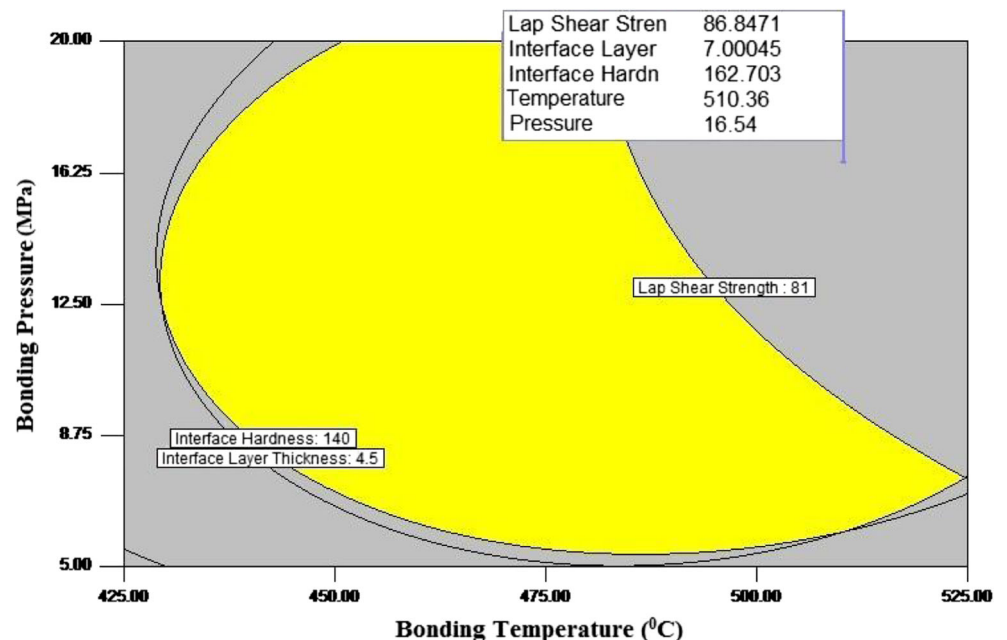
Table 10 Validation test results

Experimental details				Results			
Input parameters				Responses			
Exp. no.	Bonding temperature (°C)	Bonding pressure (MPa)	Holding time (min)		SS (MPa)	IFL (μm)	H (HV)
1	514	15	37	Actual	82	7.12	157
				Predicted	86.82	7.00	162.70
				Error%	5.55	−1.85	3.5
2	489	13	33	Actual	72	7.2	150
				Predicted	69.56	7.75	158.25
				Error%	−3.50	7.09	5.21
3	495	14	34	Actual	78	7.18	155
				Predicted	81	7.92	164.98
				Error%	3.70	9.34	6.04

gradually at the bond region of dissimilar metal joints with increasing the temperature. The particle distribution of inter-metallic compounds has no harmful effects on the joint performances.

4.3 Microhardness

Microhardness was measured across the interface of cp-Ti/AA 7075 joints (perpendicular to the diffusion layer) at the different locations, and the results are presented in Fig. 14. Hardness is maximum at the interface, irrespective of thickness of the diffusion layer. This may be due to the formation of inter-metallic compounds at the interface. In similar studies, researchers [33, 34] bonded varies materials by diffusion bonding at different temperatures. Thick diffusion layer recorded maximum hardness at all locations. This may be due to higher level of bonding temperature, bonding pressure, and holding time used to fabricate the joints. Very near to the interface region (approximately 1 mm from the interface region on both the sides), an appreciable reduction in hardness was recorded in all the joints. This may be due to the depletion of respective atoms, which are diffused into the interface region to form intermetallic compounds. Micrograph as shown in Fig. 14 depicts indentation marks at the interface.

4.4 Multi-response optimization

In this investigation, two criteria were implemented to maximize both shear strength and hardness in range of interface layer thickness. Table 7 summarizes these two criteria, while Tables 8 and 9 present the optimal solution based on the two optimization criteria as determined by Design-Expert software. In the first criterion, bonding temperature, bonding pressure, holding time, and interface layer thickness are in range, and the shear strength and interface hardness are at maximum. In the second criterion, bonding temperature, lap shear

strength, and interface hardness are in maximum range, and bonding pressure and holding time are within range, but a target of 7 μm is fixed for interface layer thickness. Table 9 presents the optimal bonding conditions, according to the second criterion that would lead to the shear strength of 87 MPa, interface layer thickness of 7 μm, and hardness of 163 HV. The result of graphical optimization is the overlay plots. This type of plots is extremely practical for quick technical use in the workshop to choose the values of bonding parameters that would achieve certain response values. Figures 15 and 16 show the processing maps (overlay plots) for criteria 1 and 2. From the maps, the yellow-shaded areas are the regions that meet the proposed criteria. These will act as reference maps for design engineers.

4.5 Validation of the developed models

To validate the developed models, three confirmation experiments were carried out with DB conditions chosen randomly from the optimization results. For the actual responses, the average of three measured results was calculated. Table 10 summarizes the experiments condition, the average of actual experimental values, the predicted values, and the percentages of error. The optimum value of process parameter and the average shear strength of diffusion-bonded joint cp-Ti/Al 7075 were found to be 87 MPa which shows the excellent agreement with the predicted values. From Fig. 11b, it is evident that the optimum diffusion layer thickness and micro-structure show the finer grains, and there is no defect in the bond region as compared with base metal micrographs (Fig. 2a, b). The validation results demonstrated that the predicted models developed are quite accurate as the percentages of error in prediction were in good agreement, with the experimental values. However, the predicted model can only be used in the parameter ranging from bonding temperature (425 to 525 °C), bonding pressure (5 to 20 MPa), and holding

time (5 to 45 min) for diffusion bonding of Cp-Ti and AA 7075 aluminum alloy only.

5 Conclusions

1. The diffusion bonding process parameters were optimized using desirability function solving the multi-response optimization to obtain the maximum strength, maximum hardness, and optimum range of interface layer thickness.

2. A maximum shear strength of 87 MPa was achieved under the bonding pressure of 15 MPa, bonding temperature of 510 °C, and holding time of 37 min. Under these processing conditions, interface layer thickness was optimum (7 μm) and hardness was maximized (163 HV).

3. Empirical relationships were developed using statistical tools such as design of experiments, regression analysis, and analysis of variance to predict the shear strength (SS), interface hardness (IH), and interface layer thickness (ILT) of FSW joints of aluminum alloys at 95 % confidence level.

4. From the ANOVA test results, it was found that bonding temperature has a great influence on bonding characteristic followed by bonding pressure and holding time.

5. Developed processing maps (overlay plots) will act as reference maps to predict the output responses.

References

1. Lee MK, Lee JG, Choi YH, Kim DW (2010) Interlayer engineering for dissimilar bonding of titanium to stainless steel. Mater Lett 64:1105–1108

2. Kenevisi MS, Mousavi Khoie SM (2012) An investigation on microstructure and mechanical properties of Al7075 to Ti–6Al–4V transient liquid phase (TLP) bonded joint. Mater Des 38:19–25

3. Alhazaa AN, Khan TI (2010) DB of Al7075 to Ti–6Al–4V using Cu coatings and Sn–3.6Ag–1Cu interlayers. J Alloys Compd 494:351–358

4. Mahendran G, Balasubramanian V, Senthilvelan T (2009) Developing diffusion bonding windows for joining AZ31B magnesium-AA2024 aluminium alloys. Mater Des 30:1240–1244

5. Mahendran G, Balasubramanian V, Senthilvelan T (2009) Developing diffusion bonding windows for joining AZ31B magnesium and copper alloys. Int J Adv Manuf Technol 42:689–695

6. Feng JC, Zhang BG, Qian YY, He P (2002) Microstructure and strength of diffusion bonded joints of Ti Al base alloy to steel. Mater Charact 48:401–406

7. Hosung LEE, Jonghoon YOON, Yeongmoo YI (2007) Oxidation behavior of titanium alloy under diffusion bonding. Thermochim Acta 455:105–108

8. Arik H, Aydin M, Kurt A, Turker M (2005) Weldability of Al4C3-Al composites via diffusion welding technique. Mater Des 26:555–560

9. Tanabe J, Sasaki T, Kishi S (2007) Diffusion bonding of Ti/graphite and Ti/diamond by hot isostatic pressing method. J Mater Process Technol 192:453–458

10. Sheng GM (2005) An experimental investigation of phase transformation superplastic diffusion bonding of titanium alloy to stainless steel. J Mater Sci 40:6385–6390

11. Myers RH, Montgomery DC (1995) Response surface methodology. Wiley, New York

12. Gunaraj V, Murugan N (1999) Application of response surface methodology for predicting weld bead quality insubmerged arc welding of pipes. J Mater Process Technol 88:266–275

13. Elangovan S, Venkateswaran P (2012) Experimental investigations on optimization of ultrasonic welding parameters for copper to brass joints using response surface method and genetic algorithm. Int J Adv Eng Rese Stud 1:55–64

14. Rajakumar S, Muralidharan C, Balasubramanian V (2011) Statistical analysis to predict grain size and hardness of the weld nugget of friction stir welded AA6061-T_6 aluminium alloy joints. Int J Adv Manuf Technol 57:151–165

15. Liu P, Li Y, Haoran G, Juan W (2006) Investigation of interfacial structure of Mg/Al vacuum diffusion-bonded joint. Vacuum 80:395–399

16. Li Y, Liu P, Wang J, Ma H (2008) XRD and SEM analysis near the diffusion bonding interface of Mg/Al dissimilar materials. Vacuum 82:15–19

17. Liu P, Li Y, Haoran G, Wang J (2005) A study of phase constitution near the interface of Mg/Al vacuum diffusion bonding. Mater Lett 59:2001–2005

18. Atasoy E, Kahraman N (2008) Diffusion bonding of cp-Ti to low carbon steel using a silver interlayer. Mater Charact 59:1481–1490

19. Husain MM, Ghosh M (2013) Inhibition of intermetallic formation during diffusion bonding of high-carbon steel. Inhibition of intermetallic formation during diffusion bonding of high-carbon steel. Int J Adv Manuf Technol 66:1871–1877

20. Sozhamannan GG, Balasivanandha Prabu S (2009) Evaluation of interface bonding strength of 6061 aluminium/silicon carbide. Int J Adv Manuf Technol 44:385–388

21. Montgomery DC (1984) Design and analysis of experiments, 2nd edn. Wiley, New York

22. Rajakumar S, Muralidharan C, Balasubramanian V (2010) Establishing empirical relationships to predict grain size and tensile strength of friction stir welded AA 6061-T6 aluminium alloy joints. Trans Nonferrous Metals Soc China 20:1863–1872

23. Rajakumar S, Balasubramanian V (2011) Multi-response optimization of friction-stir-welded AA1100 aluminium alloy joints. Int J Mat Eng Perform: 1059–1095

24. Periyasamy P, Mohan B, Balasubramanian V, Rajakumar S, Venugopal S (2012) Multi-objective optimization of friction stir welding parameters using desirability approach to join Al/SiCp metal matrix composites. Trans Nonferrous Metals Soc China 23:942–945

25. Design-Expert software (2012) V8, user's guide. Technical manual, Stat-Ease Inc., Minneapolis, MN

26. Joseph Fernandus M, Senthilkumar T, Balasubramanian V, Rajakumar S (2012) Optimising diffusion bonding parameters to maximize the strength of AA6061 aluminium and AZ31B magnesium alloy joints. Mater Des 33:31–41

27. Balasubramanian M, (2015) Characterization of diffusion-bonded titanium alloy and 304stainless steel with Ag as an interlayer, Int J Adv Manuf Technol doi:10.1007/s00170-015-7376–82

28. Mahendran G, Balasubramanian V, Senthilvelan T (2010) Influences of diffusion bonding process parameters on bond characteristics of Mg-Cu dissimilar joints. Trans Nonferrous Metals Soc China 20:997–1005

29. Kundu S, Ghosh M, Laik A, Bhanumurthy K, Kale GB, Chatterjee S (2005) Diffusion bonding of cp-Ti to 304 SS using copper interlayer. Mater Sci Eng A 407:154–160

30. Vigraman T, Ravindran D, Narayanasamy R (2012) Effect of phase transformation and intermetallic compounds on the microstructure and tensile strength properties of diffusion-bonded joints between Ti-6Al-4V and AISI 304L. Mater Des 36:714–727

31. Wu YE, Loy L (2002) Surface protection for AA 8090 aluminium alloy by diffusion bonding. J Theor Appl Fract Mech 38:71–79

32. Somekawa H, Watanabe H, Mukai T, Higashi K (2003) Low temperature diffusion bonding in a superplastic AZ31 magnesium alloy. Scr Mater 48:1249–1254

33. Naci Kurgan (2014) Investigation of the effect of diffusion bonding parameters on microstructure and mechanical properties of 7075 aluminium alloy. Int J Adv Manuf Technol 71:2115–2124

34. Kolukisa S (2007) The effect of the welding temperature on the weldability in diffusion welding of martinsitic (AISI-420) stainless steel with ductile (Spheroidal graphite-nodular) cast iron. J.Mater.Process Technol 86:33–36